(NASA-TM-72863) STABILITY AND CONTROL DERIVATIVE ESTIMATES OBTAINED FROM FLIGHT DATA FOR THE BEECH 99 AIRCRAFT (NASA) 38 p HC A03/MF A01 CSCL 01C

N79-20134

Unclas
G3/08 17241

NASA Technical Memorandum 72863

STABILITY AND CONTROL DERIVATIVE ESTIMATES OBTAINED FROM FLIGHT DATA FOR THE BEECH 99 AIRCRAFT

Russel R. Tanner and Terry D. Montgomery

April 1979

NASA

NASA Technical Memorandum 72863

STABILITY AND CONTROL DERIVATIVE ESTIMATES OBTAINED FROM FLIGHT DATA FOR THE BEECH 99 AIRCRAFT

Russel R. Tanner and Terry D. Montgomery

Dryden Flight Research Center
Edwards, California

NASA
National Aeronautics and
Space Administration

STABILITY AND CONTROL DERIVATIVE ESTIMATES
OBTAINED FROM FLIGHT DATA FOR
THE BEECH 99 AIRCRAFT

RUSSEL R. TANNER AND TERRY D. MONTGOMERY
DRYDEN FLIGHT RESEARCH CENTER

INTRODUCTION

Reliable estimates of stability and control derivatives are essential for flight simulations and handling quality evaluations of aircraft. In response to the growing need for reliable derivative estimates, the NASA Dryden Flight Research Center developed a technique for obtaining the stability and control derivatives of aircraft from flight data (ref. 1) and developed a set of FORTRAN computer programs to implement the technique (ref. 2). This method of derivative extraction is based on a modified maximum likelihood estimator that uses the Newton-Balakrishnan algorithm to perform the required minimization.

These computer programs were used to determine the stability and control derivatives of a modified Beech 99 airplane. The aircraft, flown as a cooperative effort by NASA, Beech Aircraft Corporation, and the University of Kansas Flight Research Laboratory, was utilized to study the effects of separate surface stability augmentation (ref. 3). Data were obtained with the aircraft in a clean configuration and with one-third flap deflection. This report presents the Beech 99 derivative estimates obtained with the modified maximum likelihood technique and compares these estimates with predicted values.

SYMBOLS

A, B, C, D, R	System matrices
a_n, a_x, a_y	normal, longitudinal, and lateral accelerations, g
b	reference span, m
C_L, C_D	coefficients of lift and drag
C_ℓ, C_m, C_n	coefficients of roll, pitch, and yaw moment
C_N, C_Y	coefficients of normal and lateral force
CG	center of gravity
c	mean aerodynamic chord, m
G	measurement noise spectral density matrix
g	acceleration due to gravity, m/sec^2
I_X, I_{XZ}, I_Y, I_Z	moments of inertia, kg - m^2
J	cost functional
m	mass, kg
p	roll rate, deg/sec
q	pitch rate, deg/sec
$\bar{q}$	dynamic pressure, N/m^2
r	yaw rate, deg/sec
S	wing area, m^2
t	time, sec
T_c	thrust coefficient
T	total time, sec
u	control vector
V	velocity, m/sec

W	weight, kN
X, Y, Z	longitudinal, lateral, and normal axes
XAN, XAY	distances of an and ay accelerometers forward of center of gravity, m
x	state vector
Y_ξ	computed observation vector
ZAY	distance of a_y accelerometer below center of gravity, m
z	measured observation vector
α	angle of attack, deg
β	angle of sideslip, deg
δ_a, δ_e, δ_r	aileron, elevator, and rudder deflections, deg
η	measurement noise vector
θ	pitch attitude, deg
ξ	vector of unknowns
ϕ	roll attitude, deg

Subscripts:

p, q, r, α, β, δ_a, δ_e, δ_r	derivative with respect to indicated quantity
0	bias

Superscripts:

*	matrix transpose

DESCRIPTION OF THE AIRPLANE AND INSTRUMENTATION

The modified Beech 99 airplane used in this analysis is a 14-seat, twin turboprop commercial airliner with low wings and retractable landing gear (figs. 1 and 2). Tables 1 and 2 list important geometric and mass characteristics of the Beech 99 airplane. The test airplane was modified so that there were two independently operable control surfaces where there is normally only one; however, only one set of rudder, aileron and elevator surfaces was used during the test flight. The extra surfaces are shaded in figure 1. These extra surfaces remained in fixed positions during the flight.

The instrumentation of the airplane consisted of a standard package used for the measurement of stability and control parameters, including three-axis angular rate gyros, attitude gyros, and linear accelerometers, along with boom-mounted angle of attack and angle of sideslip es. The data were filtered with 40-hertz passive analog filters, then sampled with a 9-bit pulse code modulation (PCM) system and telemetered to a ground station for real-time monitoring.

The analysis used in the derivative extraction accounts for the effect of instrument location on the measurement of linear accelerations and flow angles. The instrument locations used in the analysis of the flight data are presented in table 3. Table 4 lists the resolutions of the instrumentation system used in the analysis.

TEST PROCEDURES AND FLIGHT CONDITIONS

The Beech 99 airplane was flown in the cruise configuration for half of the maneuvers analyzed and at one-third flap setting for the remainder. All maneuvers were flown with the center of gravity at approximately 26 percent of the mean aerodynamic chord. Most of the maneuvers performed were simple aileron, rudder, or elevator pulses.

All data were obtained during a 2-hour flight in smooth air. Fifty-six maneuvers were performed for derivative estimation over an angle of attack r. 'e from 1.5 to 4.5 degrees, a velocity range from 65 to 100 meters per second and an altitude range from 1800 to 3200 meters. Table 5 lists the flight condition corresponding to each maneuver.

METHOD OF ANALYSIS

A maximum likelihood method of analysis was used to determine a complete set of linear body axis stability and control derivatives from the 56 maneuvers performed in flight. The digital computer program used is called the modified maximum likelihood estimator, version three (MMLE-3) which is an outgrowth of the program described in detail and listed in reference 2. The program is discussed briefly in appendix A. Further information is available upon request from the Dryden Flight Research Center. The analysis technique is an iterative technique that minimizes the difference between the measured aircraft response and the computed aircraft response by adjusting the stability and control derivative values used in calculating the computed response. This method can be modified to include á priori information from previous calculations, flight tests, or wind tunnel tests; however, no á priori information was used in this Beech 99 analysis. The maximum likelihood technique is described fully in reference 1.

In addition to giving derivative estimates, this method provides uncertainty levels for each derivative. The uncertainty levels are proportional to the approximation of the Cramer-Rao bounds described in reference 1, and are analogous to the standard deviations of the estimated derivatives. The larger the uncertainty level, the more uncertain the validity of the estimated value. The uncertainty levels obtained for derivatives from different maneuvers at the same flight conditions can be compared to determine the most valid estimate. The uncertainty levels provide additional information about the validity of the derivative estimation. Further information on the interpretation of uncertainty levels is included in reference 4.

The digital computer program used in the data analysis is capable of producing one set of derivative estimates based on multiple sets of data. The lateral-directional derivative estimates in this report result from the simultaneous analysis of both rudder and aileron maneuvers. Analysis of rudder and aileron maneuvers simultaneously usually results in improved derivative estimates, as shown in reference 4.

The cost functional minimized by the program is given in appendix A. The matrix G in this cost functional acts as a signal weighting matrix. For this analysis, G was chosen to be diagonal with values given in table 6.

RESULTS AND DISCUSSION

For all 56 maneuvers flown with the Beech 99 airplane, the measured aircraft response compared satisfactorily with the computed response based on the maximum likelihood estimation. A typical longitudinal maneuver is shown in figure 3, and a typical lateral-directional double maneuver is shown in figure 4. The measured (solid-line) and computed (dashed line) response of the aircraft are in excellent agreement in these figures. Some maneuvers produced better agreement than others; however, on the average, the agreement was quite good.

An atypical maneuver combining aileron and rudder inputs is shown in figure 5. This maneuver was performed to determine any nonlinearities in aileron effectiveness. The excellent fit in figure 5 based on a linear model indicates that there was no significant nonlinearity in aileron effectiveness. The MMLE stability and control derivative estimates based on the analysis of this maneuver were in excellent agreement with estimates from more conventional maneuvers. The analysis of this maneuver required that the small angle approximation (in bank angle) be removed from the mathematical model (see appendix B). All other maneuvers were analyzed using small angle approximations.

The estimates for 56 maneuvers (19 primarily with elevator inputs, 21 primarily with rudder inputs, 15 primarily with aileron inputs, and one with simultaneous aileron and rudder inputs) are presented in figures 6 and 7.

The longitudinal stability and control derivative estimates are presented in figure 6, while the lateral-directional estimates are displayed in figure 7. Each symbol indicates the derivative estimate for one maneuver, and the vertical bar associated with the symbol represents the uncertainty level for that derivative estimate. The square symbols are used to indicate one-third flap down maneuvers. Manufacturer predicted derivatives based on a combination of analytical predictions, wind tunnel tests, and flight test results are shown along with the MMLE-3 derivative estimates for comparison.

The manufacturer's predictions of derivatives that are functions of thrust coefficient (C_{N_α}, $C_{N_{\delta_e}}$, $C_{m_{\delta_e}}$, and C_{n_β}) are indicated by dashed lines for thrust coefficients of 0 and 0.1. This range of thrust coefficients includes the values observed in flight (see table 3). The manufacturer's predictions for the derivatives that are not functions of thrust coefficient are indicated by a single dashed line. These predictions are valid for both cruise and one-third flap down configurations. Details of the mathematics involved in the presentation of the manufacturer's derivatives are given in appendix B.

LONGITUDINAL DERIVATIVES

Figure 6 shows the MMLE-3 longitudinal derivative estimates for the Beech 99 aircraft along with the corresponding predictions of the manufacturer. Comparison between the flight estimates and the manufacturers predictions shows close agreement except for the derivative C_{m_α}. For some unexplained reason, the flight data did not produce consistent estimates of this derivative. Other flight estimated derivatives are consistent, with the exception of the estimates of C_{m_q} and $C_{m_{\delta_e}}$ resulting from one maneuver at an angle of attack of 4.25 degrees. The plots of C_{N_α}, C_{m_q}, $C_{N_{\delta_e}}$, and $C_{m_{\delta_e}}$ are nearly constant with angle of attack, showing no observable effect of flap deflection. All these parameters show good agreement with the manufacturer's estimates.

LATERAL-DIRECTIONAL DERIVATIVES

As with the longitudinal derivatives, the lateral-directional derivatives are plotted with the manufacturer's estimates (fig. 7). The derivatives C_{ℓ_β}, C_{ℓ_p}, C_{n_p}, C_{ℓ_r}, C_{n_r}, $C_{Y_{\delta_a}}$, $C_{Y_{\delta_r}}$, $C_{\ell_{\delta_r}}$, and $C_{n_{\delta_r}}$ are quite consistent with the derivative estimates of the manufacturer. $C_{\ell_{\delta_a}}$ is for the most part smaller than the manufacturer's estimates, while C_{n_β} and C_{Y_β} are consistently larger in magnitude than the manufacturer's estimates for both cruise and one-third flap configurations. On the whole, the lateral-directional derivative estimates are repeatable and show consistent trends with angle of attack.

CONCLUDING REMARKS

A complete set of linear stability and control derivatives for a Beech 99 airliner was determined using a modified maximum likelihood estimator. The derivatives were extracted for both the longitudinal and lateral-directional modes. The maneuvers were flown in smooth air at angles of attack ranging from 1.5 to 4.5 degrees. The first 29 maneuvers were flown in the cruise configuration and the last 27 were flown in a one-third flap down configuration. The one-third flap down configuration had little effect on most of the stability and control derivative estimates. All 56 maneuvers produced satisfactory results. In general, derivative estimates from flight data for the Beech 99 airplane were quite consistent with the manufacturer's predictions, which are based on a combination of wind tunnel data, analytical estimates, and flight test data.

Dryden Flight Research Center
National Aeronautics and Space Administration
Edwards, CA, November 27, 1978

APPENDIX A

MAXIMUM LIKELIHOOD ESTIMATION PROGRAM AND EQUATIONS OF MOTION

The analysis for this report was done with the MMLE-3 computer program, an outgrowth of the MMLE program (ref. 2). MMLE-3 is a general maximum likelihood estimation program used at the Dryden Flight Research Center. This section briefly describes the features of MMLE-3.

The maximum likelihood estimates are determined by minimizing the difference between the aircraft measured response and the calculated response determined by integrating the aircraft equations of motion. This response difference is formulated as a cost functional (discussed below). The minimization of this functional is performed by varying the aerodynamic coefficients in the aircraft equations of motion.

In general form, the equations of motion are:

$$R(t)\,\dot{x}(t) = A(t)\,x(t) + B(t)\,u(t)$$

$$y(t) = C(t)\,x(t) + D(t)\,u(t) + G\eta(t)$$

The system matrices (R,A,B,C,D) can be time functions because of the variations of $\bar{q}$, V, θ, and ϕ during the maneuvers. Time varying matrices were not used in the analysis of the Beech 99 data, except for the maneuver shown in figure 5.

The maximum likelihood estimates are obtained by minimizing the cost functional

$$J(\xi) = \int_0^T \left[y_\xi(t) - z(t)\right]^* \left(GG^*\right)^{-1} \left[y_\xi(t) - z(t)\right] \quad dt$$

where ξ is the vector of unknowns, z is the measured response, and y_ξ is the computed response based on ξ. MMLE-3 uses a Newton-Balakrishnan iterative algorithm (ref. 2) to perform the minimization.

The equations of motion used in this report are given below. In many cases, average values of parameters are used to obtain time invariant system matrices. These equations of motion use small angle approximations for β, but not for α, θ, or ϕ. Symmetry about the XZ plane is assumed. All angles in these equations are in radians. The longitudinal state equations are:

$$\dot{\alpha} = -\frac{\bar{q}S}{mV} C_L + q + \frac{g}{V}\left[(\cos\theta)\,(\cos\phi)\,(\cos\alpha) + (\sin\theta)\,(\sin\alpha)\right]$$

$$\dot{q}I_Y = \bar{q}Sc\, C_m$$

$$\dot{\theta} = q(\cos \phi)$$

The longitudinal observation vector consists of the state vector concatenated with an observation of normal acceleration. The equation used for computing normal acceleration is:

$$a_n = \frac{\bar{q}S}{mg} C_N + \frac{XAN}{g} \dot{q}$$

In expanded form, the longitudinal aerodynamic coefficients are:

$$C_N = C_{N_\alpha} \alpha + C_{N_{\delta_e}} \delta_e + C_{N_0}$$

$$C_m = C_{m_\alpha} \alpha + C_{m_q} \frac{\bar{q}c}{2V} + C_{m_{\delta_e}} \delta_e + C_{m_0}$$

and

$$C_L = C_N \text{ (for low } \alpha)$$

The lateral-directional state equations are:

$$\dot{\beta} = \frac{\bar{q}S}{mV} C_y + p(\sin \alpha) - r(\sin \alpha) + \frac{g}{V}(\cos \theta)(\sin \phi)$$

$$\dot{p}I_X - \dot{r}I_{XZ} = \bar{q}sb\, C_\ell$$

$$\dot{r}I_X - \dot{p}I_{XZ} = \bar{q}sb\, C_n$$

$$\dot{\phi} = p + r(\cos \phi)(\tan \theta)$$

The lateral-directional observation vector consists of the state vector concatenated with lateral acceleration given by:

$$a_y = \frac{\bar{q}S}{mg} C_Y - \frac{ZAY}{g} \dot{p} + \frac{XAY}{g} \dot{r}$$

In expanded form, the lateral-directional aerodynamic coefficients are:

$$C_Y = C_{Y_\beta}\beta + C_{Y_{\delta_a}}\delta_a + C_{Y_{\delta_r}}\delta_r + C_{Y_0}$$

$$C_\ell = C_{\ell_\beta}\beta + C_{\ell_p}\frac{pb}{2V} + C_{\ell_r}\frac{rb}{2V}\ C_{\ell_{\delta_a}}\delta_a + C_{\ell_{\delta_r}}\delta_r + C_{\ell_0}$$

$$C_n = C_{n_\beta}\beta + C_{n_p}\frac{pb}{2V} + C_{n_r}\frac{rb}{2V} + C_{n_{\delta_a}}\delta_a + C_{n_{\delta_r}}\delta_r + C_{n_0}$$

APPENDIX B

"MANUFACTURER'S DERIVATIVE ESTIMATES"

Reference 5 contains the manufacturer's estimates of the total force and moment coefficients of the Beech 99 aircraft. These estimates are in an analytical form which permits generation of stability and control derivatives by partial differentiation. These derivative estimates are valid for both the cruise and one-third flap configurations with the exception of the two estimates of C_{L_α}. The resulting derivative estimates are functionally dependent on the thrust coefficient. The derivative estimates and methods of the manufacturer are presented here to allow direct comparison of these estimates with flight results.

The longitudinal derivative estimates are as follows:

$$C_{L_\alpha} = 0.096 + 0.151\ T_c \text{ per deg (Cruise)}$$

$$C_{L_\alpha} = 0.101 + 0.151\ T_c \text{ per deg (1/3 flap)}$$

$$C_{m_{\alpha_{c/4}}} = 0.010 + 0.010\ T_c \text{ per deg}$$

$$C_{m_{\delta_e}} = -0.034 - 0.032\ T_c \text{ per deg}$$

$$C_{m_{\dot\alpha}} = -43.1 \text{ per rad}$$

$$C_{m_q} = -3.40 \text{ per rad}$$

The lateral-directional derivative estimates are as follows:

$$C_{n_\beta} = 0.014 - 0.0015\ T_c \text{ per deg}$$

$$C_{\ell_\beta} = -0.0023 \text{ per deg}$$

$$C_{Y_\beta} = -0.010 \text{ per deg}$$

$$C_{n_{\delta_r}} = -0.0014 \text{ per deg}$$

$$C_{\ell_{\delta_r}} = 0.00017 - 0.000022\ \alpha \text{ per deg}$$

$C_{Y_{\delta_r}}$ = 0.0025 per rad

C_{n_r} = -0.20 - 0.197α per rad

C_{ℓ_r} = +0.05 + 0.623α per rad

C_{Y_r} = 0.394 per rad

C_{n_p} = 0.0079 - 0.762α per rad

C_{ℓ_p} = -0.515 per rad

C_{Y_p} = -0.199 - 0.385α per rad

$C_{\ell_{\delta_a}}$ = 0.0027 per deg

$C_{n_{\delta_a}}$ = -0.0015 per deg

where $T_c = \frac{\text{TOTAL THRUST}}{\bar{q}S}$

At the steady state, low angle of attack conditions at which derivative extraction maneuvers were performed, the following approximations are valid:

$$C_L = \frac{W}{\bar{q}S}$$

$$T_c = C_D$$

From reference 5:

$$C_D = 0.0275 + 0.0625\ C_L^2$$

Thus,

$$T_c = 0.0275 + 0.0625 \left(\frac{W}{\bar{q}S}\right)^2$$

This equation shows that the cruise thrust coefficient is a function of dynamic pressure, q, alone, because W and S are known constants.

$$W = 39.59 \text{ kN}$$

$$S = 26 \text{ m}^2$$

Substituting these known values into the thrust coefficient equation,

$$T_c = 0.0275 + \frac{0.145}{\bar{q}^2}$$

During the Beech 99 flight, dynamic pressure varied between 2 and 5 kN/m^2. T_c ranged from approximately 0 to 0.1. With this in mind, the Beech derivative estimates for the airplane were computed at the T_c extrema, and these estimates were plotted with the flight-determined derivatives.

The derivatives $C_{m_{\alpha_{c/4}}}$ and C_{n_β} must be resolved to a flight center of gravity position of 26 percent of the mean aerodynamic chord. This is accomplished in the following equations:

$$C_{m_\alpha} = C_{m_{\alpha_{c/4}}} - C_{L_\alpha} (CG_{flight} - CG_{c/4})^1$$

$$C_{n_\beta} = C_{n_{\beta_{Beech}}} - C_{Y_\beta} (CG_{flight} - CG_{c/4})(c/b)$$

For $T_c = 0$,

$$C_{m_\alpha} = -0.0289 \text{ per deg}$$

$$C_{n_\beta} = 0.0014 \text{ per deg}$$

and for $T_c = 0.1$,

$$C_{m_\alpha} = -0.0313 \text{ per deg}$$

$$C_{n_\beta} = 0.00125 \text{ per deg}$$

[1]Reference center of gravity (CG_{flight}) is 26 percent mean aerodynamic chord.

REFERENCES

1. Iliff, Kenneth W.; and Taylor, Lawrence W., Jr.: Determination of Stability Derivatives From Flight Data Using a Newton-Raphson Minimization Technique. NASA TN D-6579, 1972.

2. Maine, Richard E.; and Iliff, Kenneth W.: A FORTRAN Program for Determining Aircraft Stability and Control Derivatives From Flight Data. NASA TN D-7831, 1975.

3. Jenks, Gerald E.; Henry, Howard F.; and Roskam, Jan: Flight Test Results for a Separate Surface Stability Augmented Beech Model 99. NASA CR-143839, 1977.

4. Iliff, Kenneth W.; and Maine, Richard E.: Practical Aspects of Using a Maximum Likelihood Estimation Method to Extract Stability and Control Derivatives From Flight Data. NASA TN D-8209, 1976.

5. Agnihotri, A.K.: Engineering Aerodynamics Report (BAR 1050) - Aerodynamic Data for KU/Beech AACS Test Bed (PD 280). Beech Aircraft Corp., Report No. E 22213 ASC, Sept. 12, 1972

TABLE 1. GEOMETRIC CHARACTERISTICS OF

BEECH 99 AIRPLANE

Wing:	
Reference area, m^2	26.01
Reference chord (mean aerodynamic chord), m	1.98
Reference span, m	13.98
Aspect ratio	7.54
Angle of sweep, deg	0
Ailerons:	
Area, (total) m^2	1.29
Chord, m	0.28
Span, (each) m	0.24
Flaps:	
Area, (total) m^2	3.51
Span, (each) m	3.78
Chord, m	0.08
Horizontal tail:	
Area, m^2	9.29
Span, m	6.82
Mean aerodynamic chord, m	1.41
Aspect ratio	5.0
Angle of sweep, deg.	17.0
Elevator:	
Area, m^2	2.45
Mean aerodynamic chord, m	0.39
Vertical tail:	
Area, m^2	4.17
Span, m	2.32
Mean aerodynamic chord, m	1.92
Aspect ratio	1.29
Angle of sweep, deg	19.5
Rudder:	
Area, m^2	1.12
Mean aerodynamic chord, m	0.55
Reference center of gravity, percent of reference chord	26.

TABLE 2. MASS DATA FOR BEECH 99 AIRPLANE

Full Fuel Condition

Mass, kg	4036.15
CG, percent of reference chord	26%
I_X, kg - m^2	16,900
I_Y, kg - m^2	23,900
I_Z, kg - m^2	38,900
I_{XZ}, kg - m^2	3,520

TABLE 3. INSTRUMENT LOCATIONS RELATIVE TO REFERENCE CENTER OF GRAVITY

Instrument	Distance Forward of Reference CG, m	Distance below reference CG, m
α	7	- - -
β	7	0
a_n	0.381	- - -
a_x	- - -	0.102
a_y	-1.5	0.102

TABLE 4. INSTRUMENT RESOLUTIONS FOR BEECH 99 DATA

Signal	Resolution
α	0.07 deg
β	0.08 deg
p	0.25 deg/sec
q	0.08 deg/sec
r	0.08 deg/sec
θ	0.18 deg
ϕ	0.35 deg
a_n	0.01g
a_x	0.002g
a_y	0.001g
δ_a	0.08 deg
δ_e	0.06 deg
δ_r	0.10 deg
V	0.07 m/sec

TABLE 5. MANEUVERS AND FLIGHT CONDITIONS

Case Number	Dynamic Pressure, kN/m^2	Thrust Coefficient	Angle of Attack, deg.	Velocity, m/sec	Flap Setting deg.
1	4.73	0.034	1.7	99	0
2	4.62	0.034	1.7	98	0
3	4.56	0.034	1.7	97	0
4/8	4.77	0.034	1.6	99	0
5/7	4.68	0.034	1.6	98	0
6/9	4.67	0.034	1.6	101	0
10	4.95	0.034	1.9	100	0
11	4.56	0.034	1.8	100	0
12	4.61	0.034	1.8	100	0
13	4.63	0.034	1.8	100	0
14/17	4.50	0.035	1.8	98	0
15/18	4.69	0.034	1.8	99	0
16/19	4.53	0.035	1.8	97	0
20	4.83	0.034	1.5	99	0
21	4.75	0.034	1.6	98	0
22	4.67	0.034	1.5	97	0
23	4.65	0.034	1.5	97	0
24/26/27	4.80	0.034	1.5	99	0
25/28/29	4.80	0.034	1.5	100	0
30	2.23	0.057	3.2	67	15
31	2.20	0.057	3.4	67	15
32	2.20	0.058	3.3	67	15
33	2.17	0.060	3.5	65	15
34/37	2.10	0.058	3.3	66	15
35/38	2.25	0.056	3.1	68	15
36/39	2.22	0.057	3.2	67	15
40	2.04	0.062	4.2	65	15
41	2.07	0.060	4.4	66	15
42	2.09	0.061	4.4	65	15
43/46	2.08	0.061	4.3	65	15
44/47	2.03	0.063	4.4	64	15
45/48	2.04	0.062	4.3	63	15
49	2.24	0.056	3.0	66	15
50	2.20	0.057	3.1	66	15
51	2.15	0.059	3.1	65	15
52/55	2.14	0.059	3.2	65	15
53/54/56	2.16	0.059	3.2	66	15

TABLE 6. WEIGHTING VALUES USED IN ANALYSIS OF BEECH 99 DATA

Signal	Diagonal element of G INVERSE
α	35 per deg
q	45 sec/deg
θ	55 per deg
a_n	300 per g
β	42 per deg
p	8.5 sec/deg
r	40 sec/deg
ϕ	15 deg
a_y	500 per g

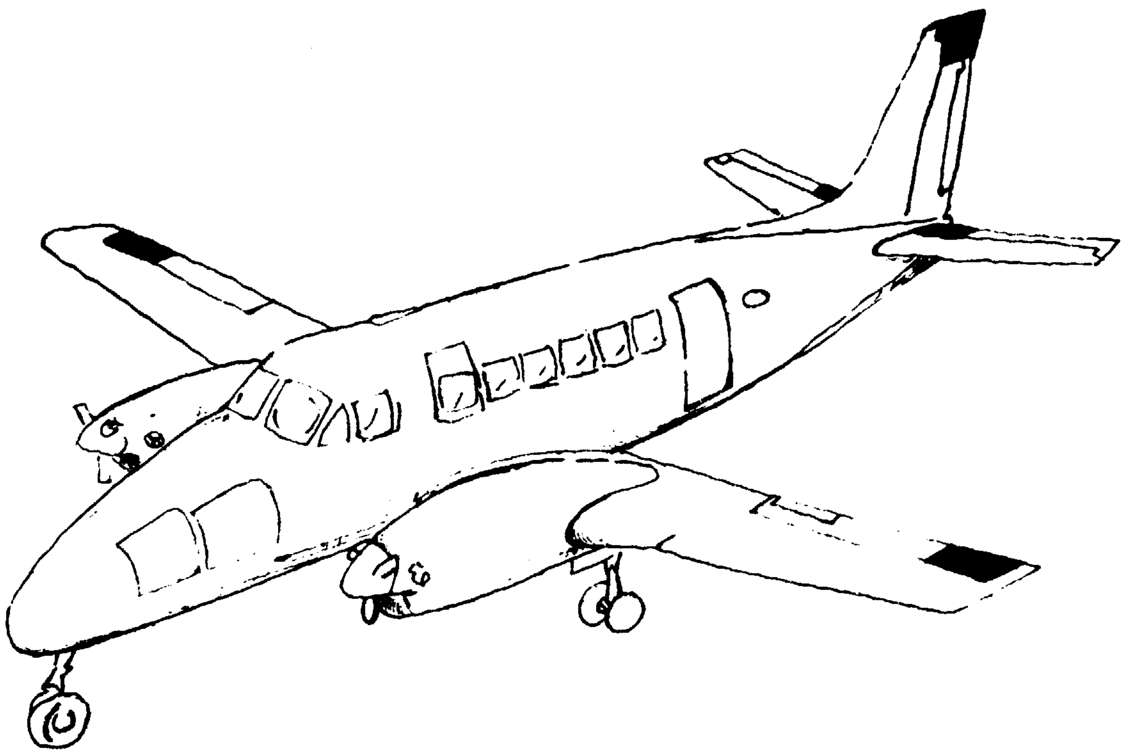

Figure 1. Beech 99 airplane. Dark areas denote extra control surfaces which remained in fixed positions during the test flight.

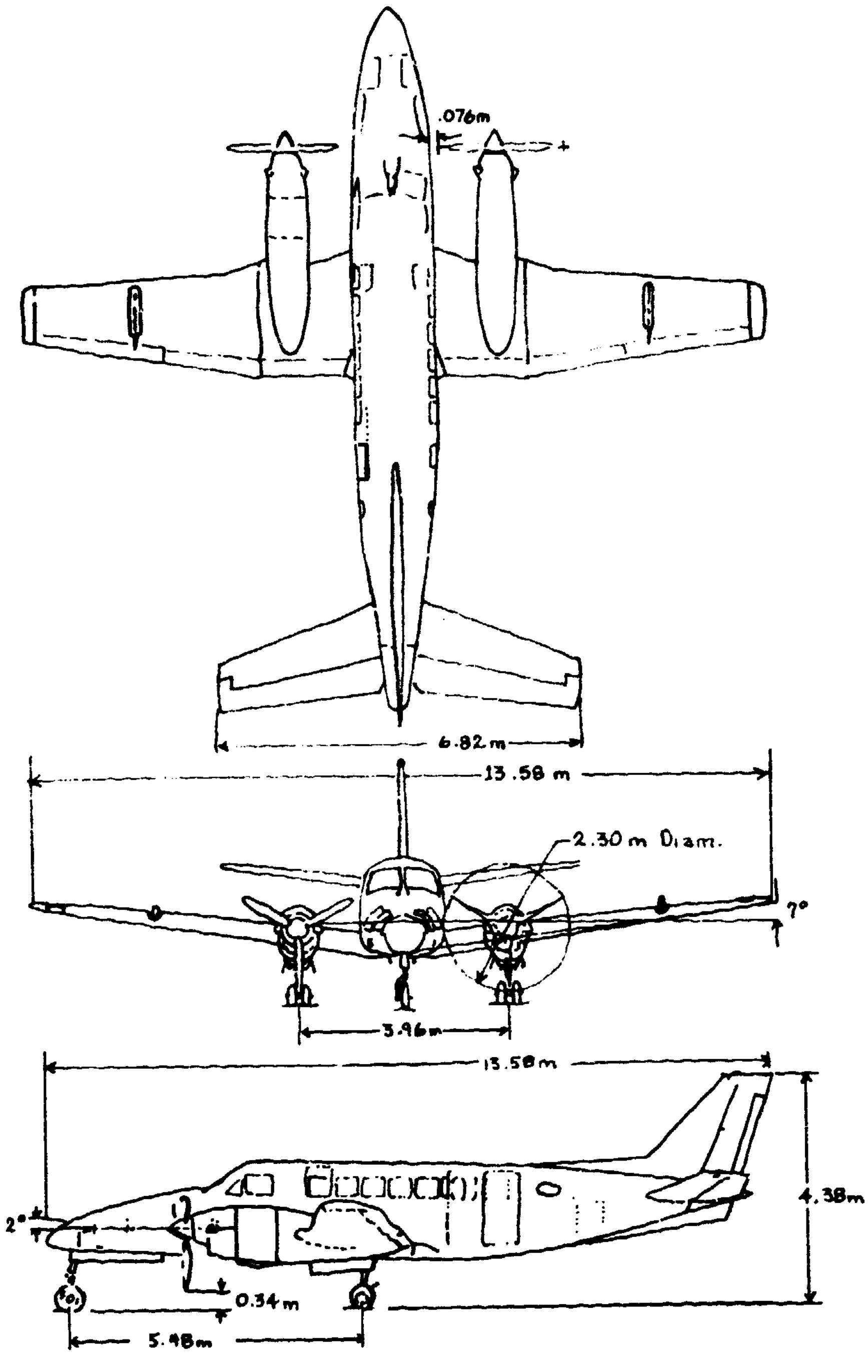

Figure 2. Three views of the Beech 99 airplane.

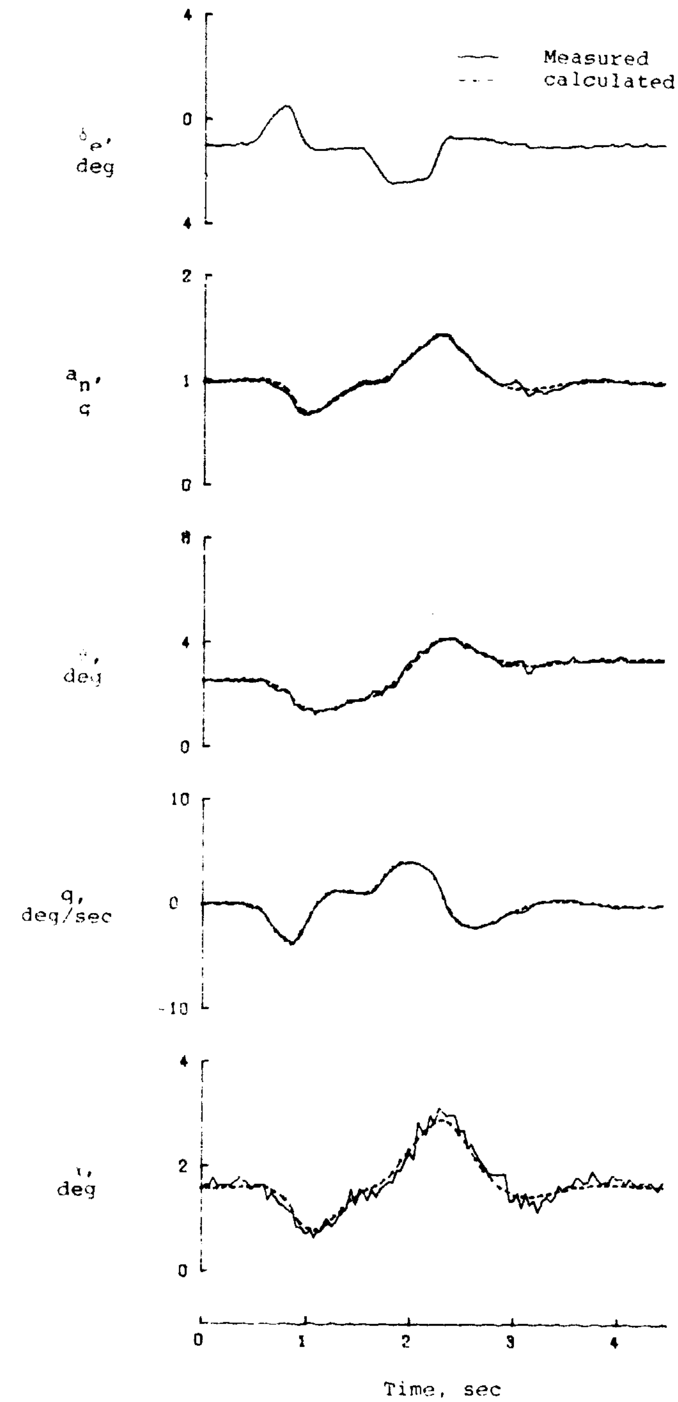

Figure 3. Typical longitudinal maneuver.

ORIGINAL PAGE IS OF POOR QUALITY

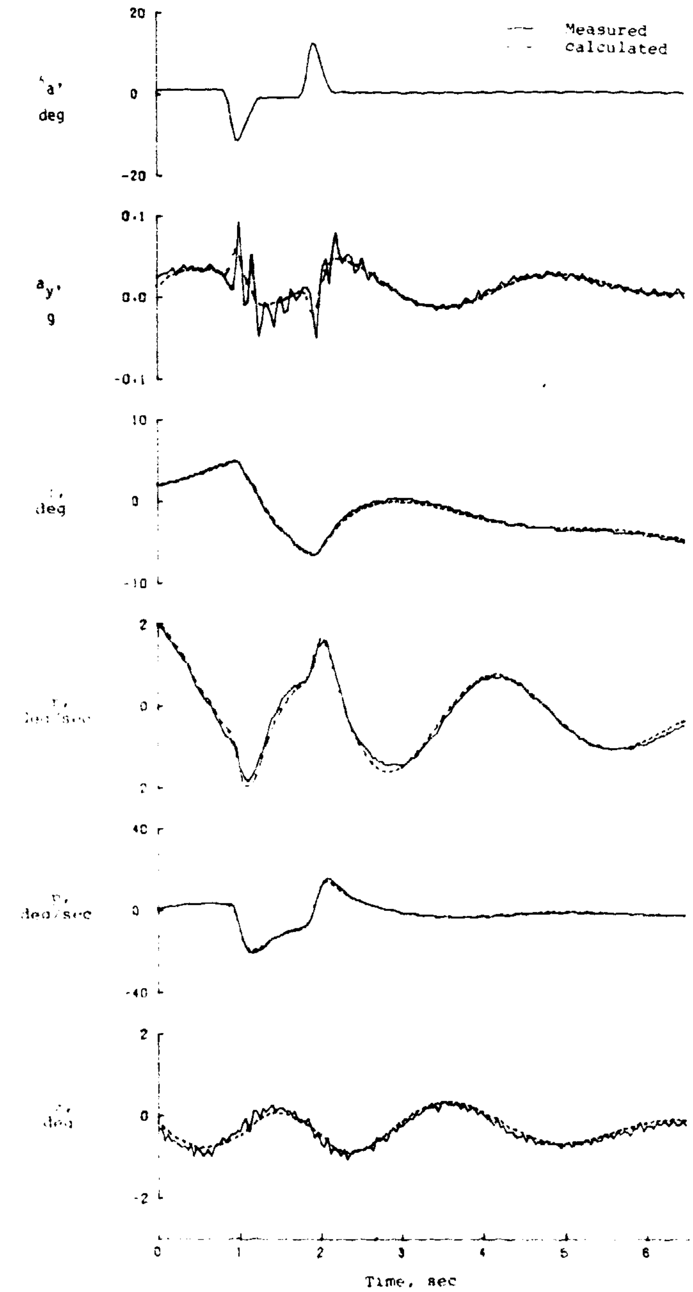

(a) Aileron doublet

Figure 4. Typical lateral-directional double maneuver.

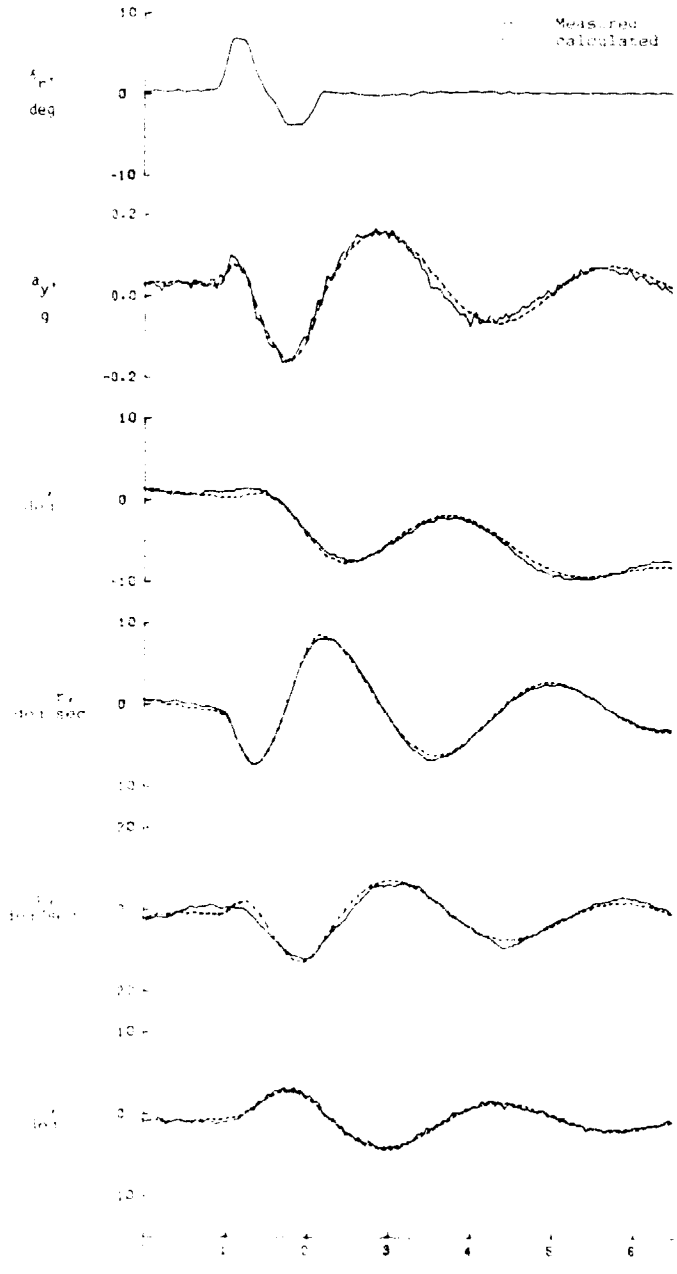

(b) Rudder doublet

Figure 4. Concluded.

ORIGINAL PAGE IS
OF POOR QUALITY

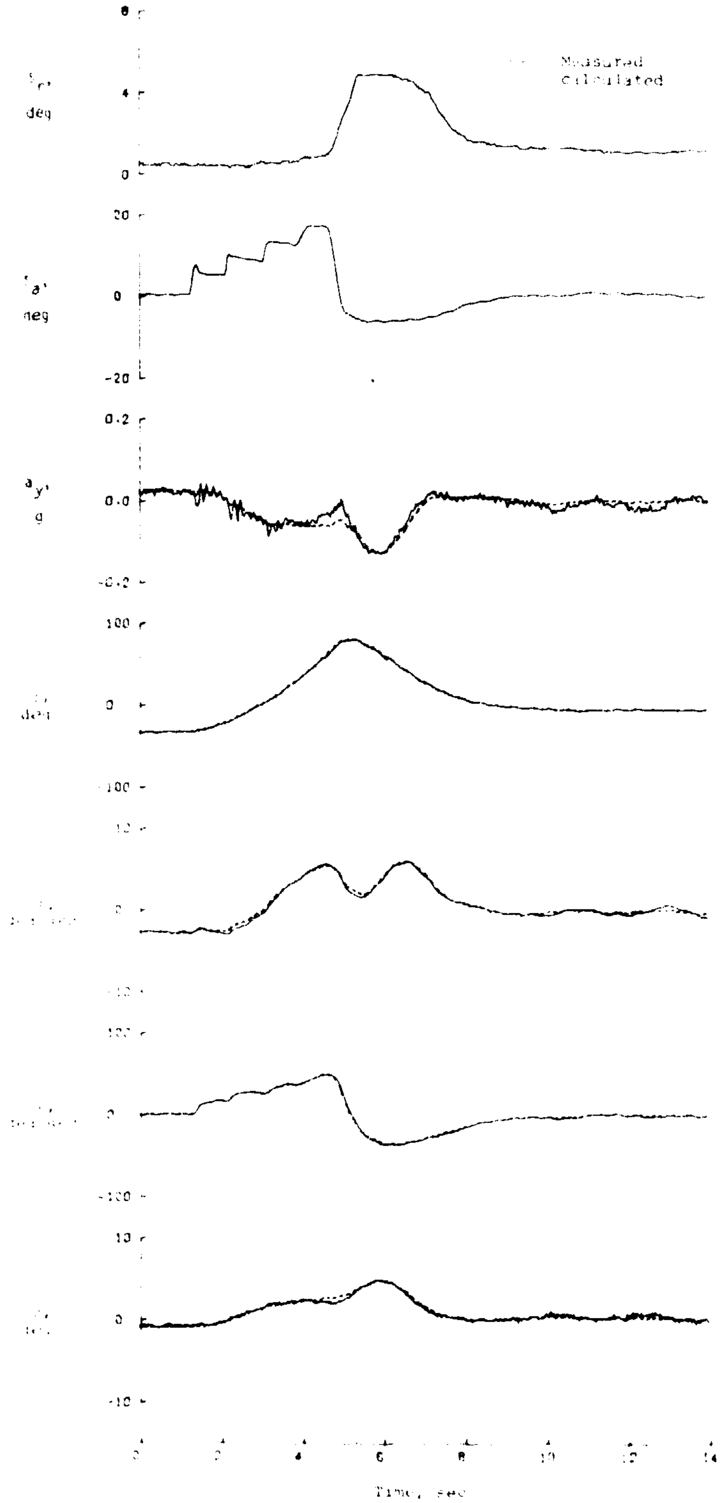

Figure [illegible]. A lateral-directional maneuver to determine nonlinear aileron effectiveness.

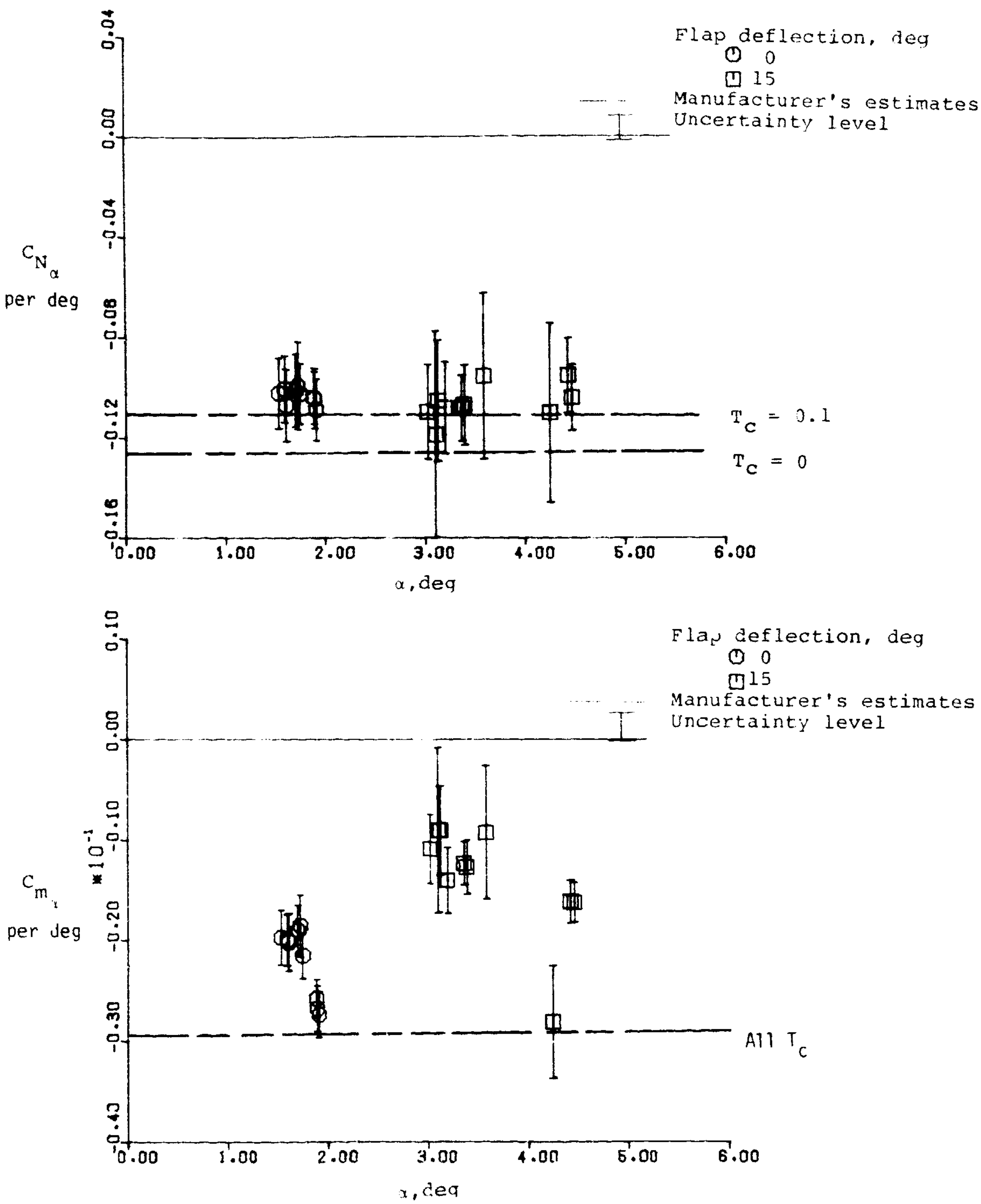

(a) C_{N_α}, C_{m_α}

Figure 6. Summary of longitudinal derivatives.

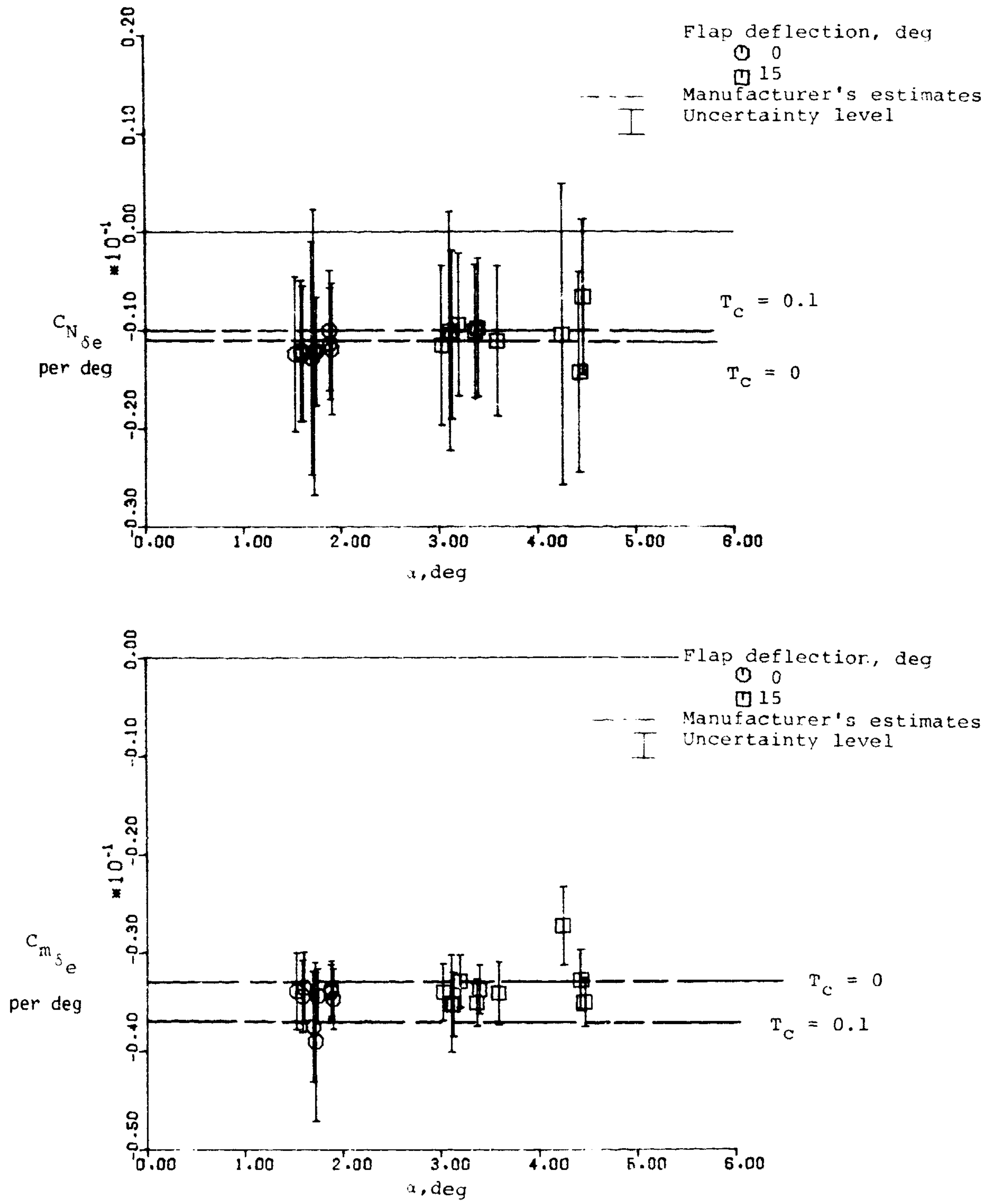

(b) $C_{N_{\delta_e}}$, $C_{m_{\delta_e}}$

Figure 6. Continued.

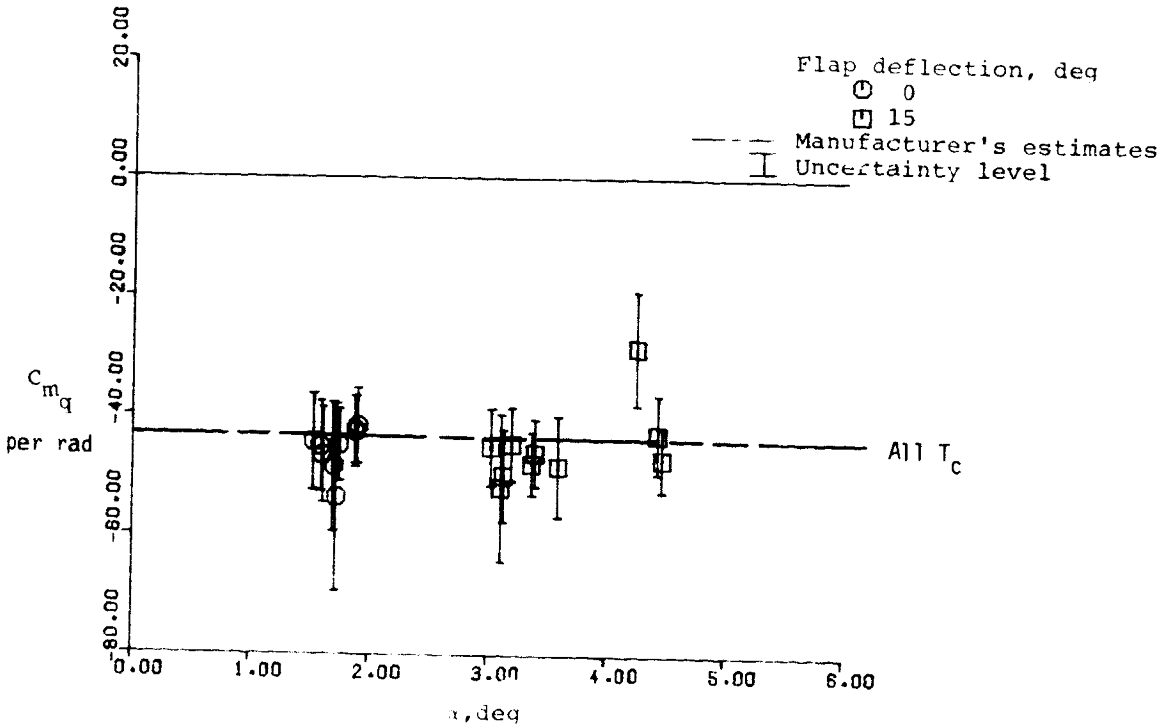

(c) C_{m_q}

Figure 6. Concluded.

ORIGINAL PAGE IS
OF POOR QUALITY

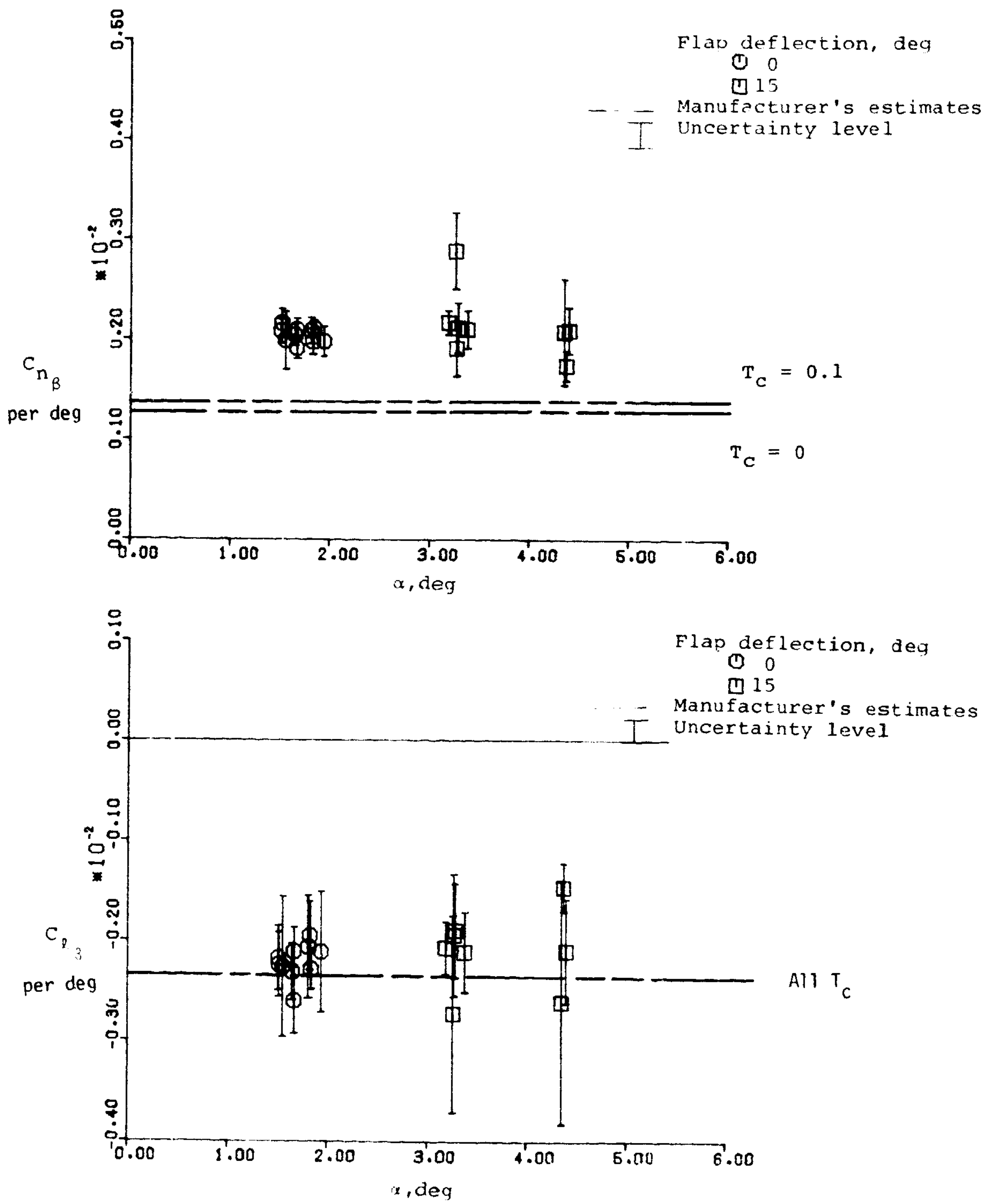

(a) C_{n_β}, C_{ℓ_β}

Figure 7. Summary of lateral-directional derivatives.

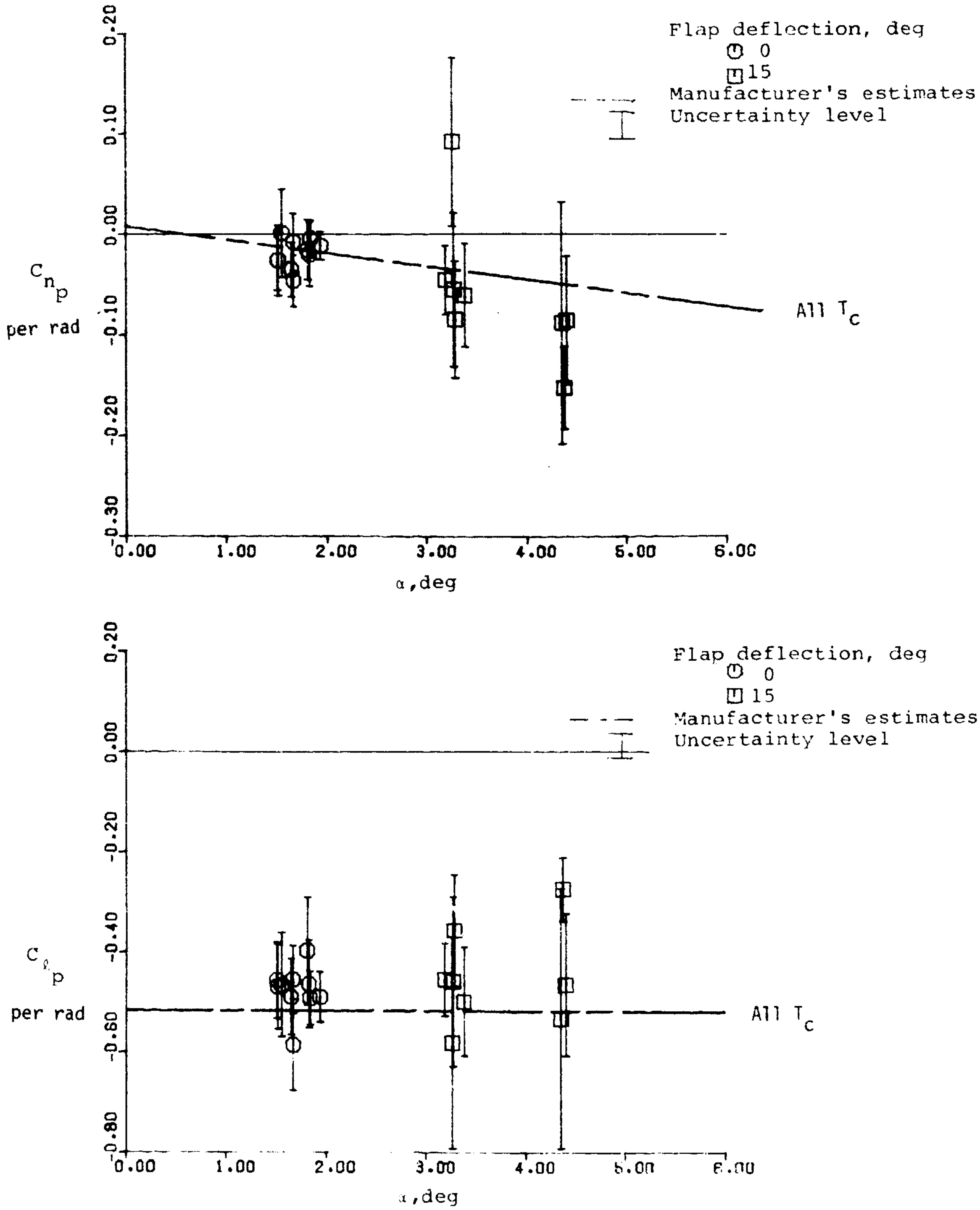

(b) C_{n_p}, C_{ℓ_p}

Figure 7. Continued.

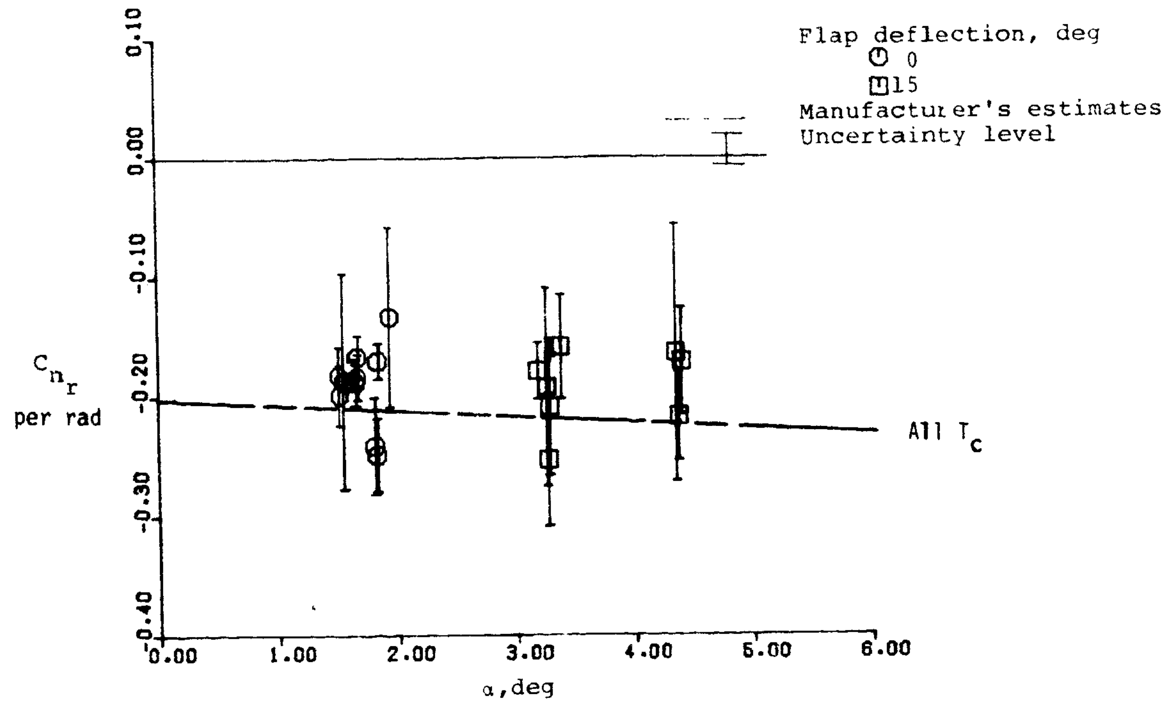

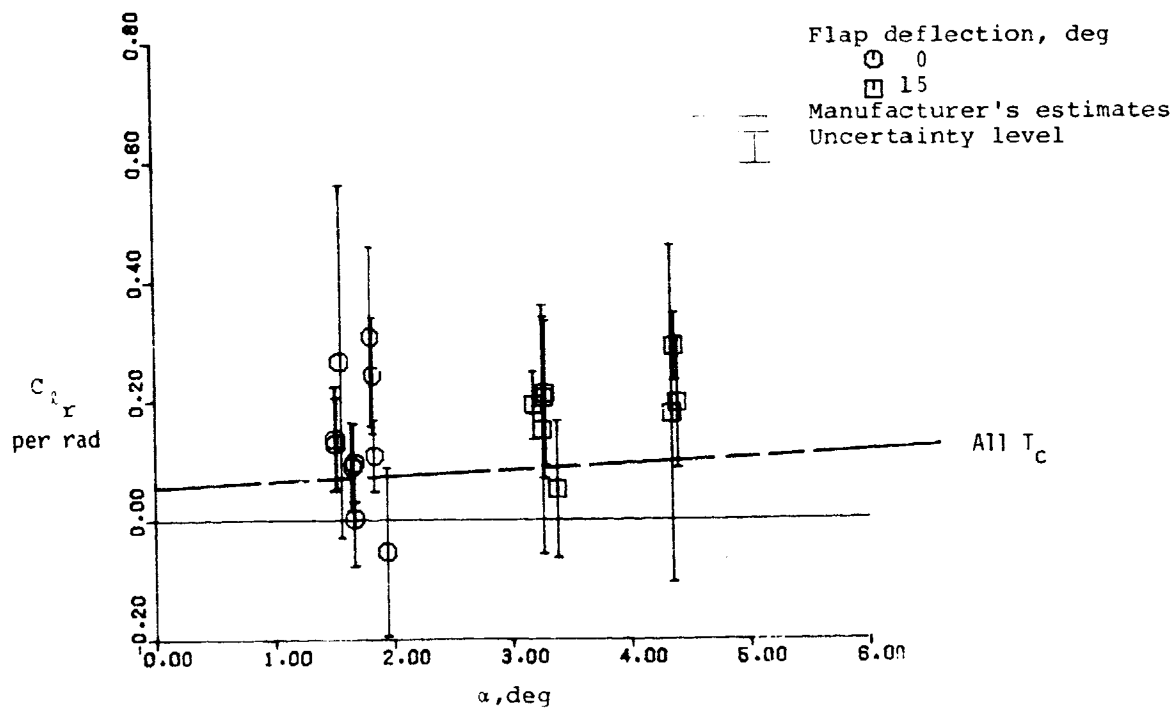

(c) C_{n_r}, C_{ℓ_r}

Figure 7. Continued.

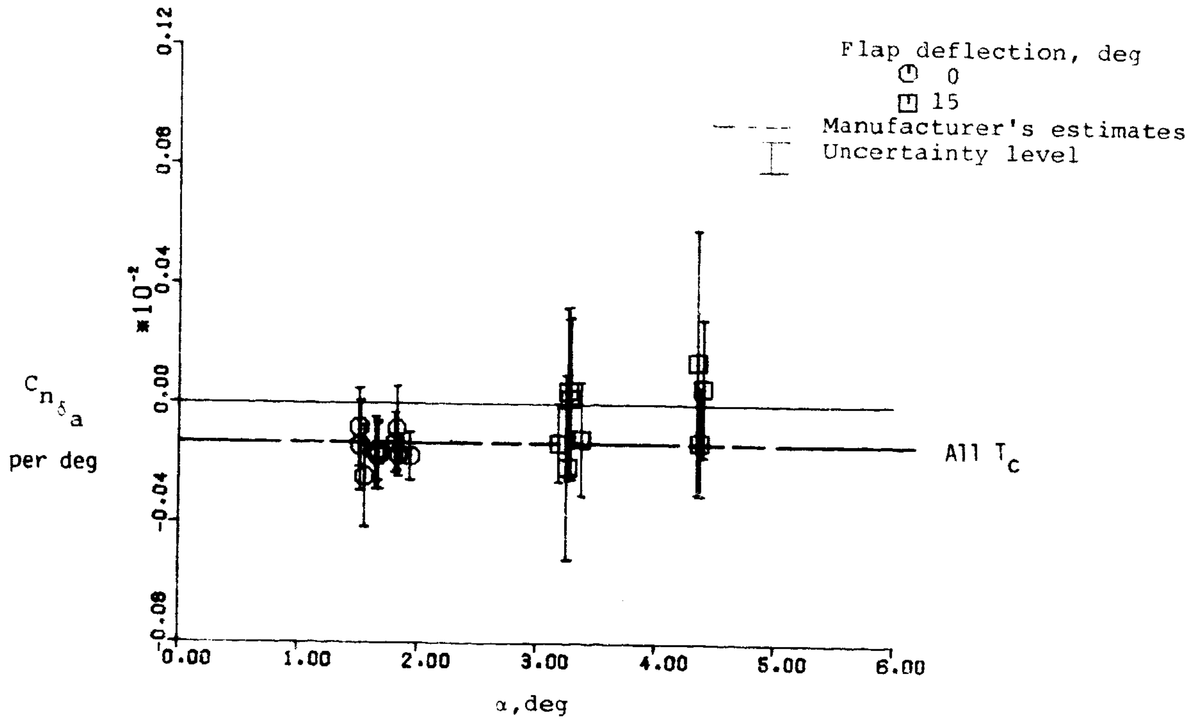

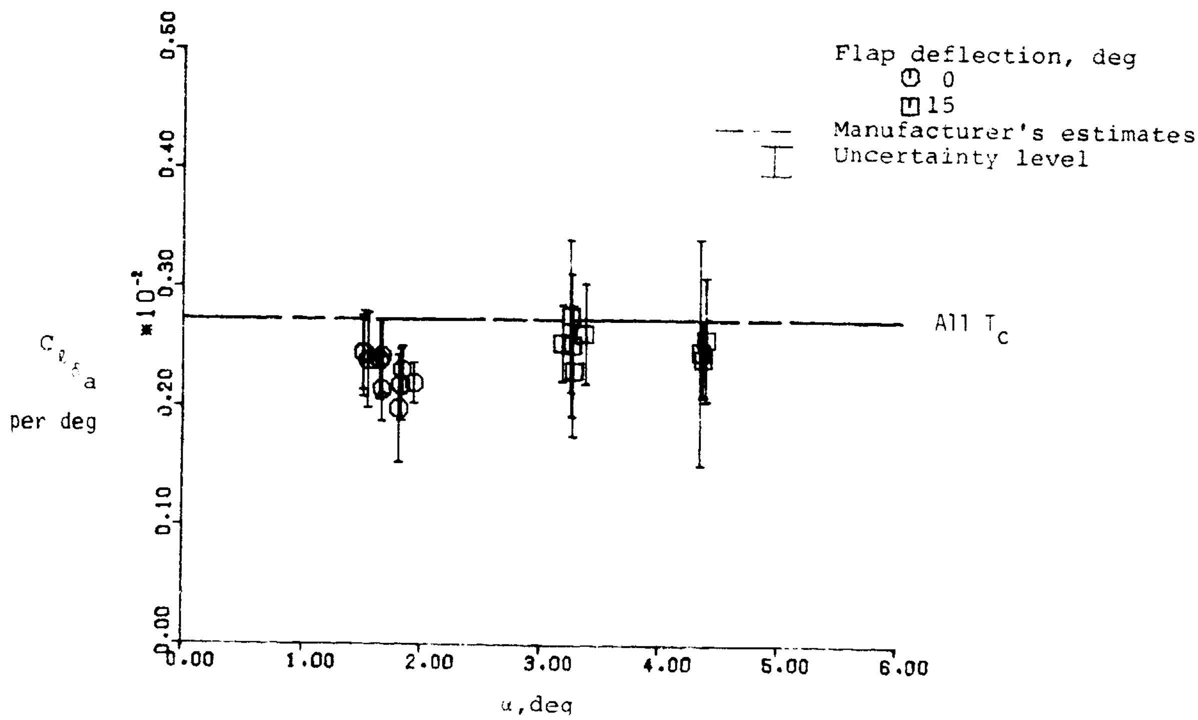

(d) $C_{n_{\delta_a}}$, $C_{\ell_{\delta_a}}$

Figure 7. Continued.

ORIGINAL PAGE IS
OF POOR QUALITY

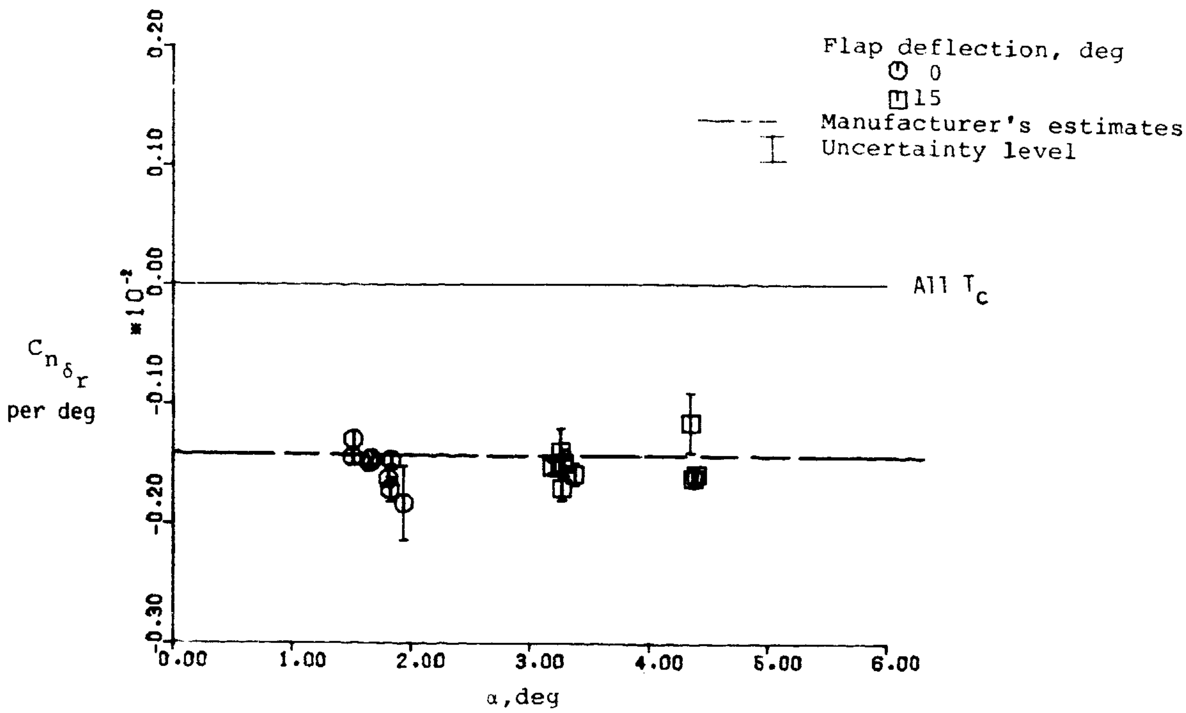

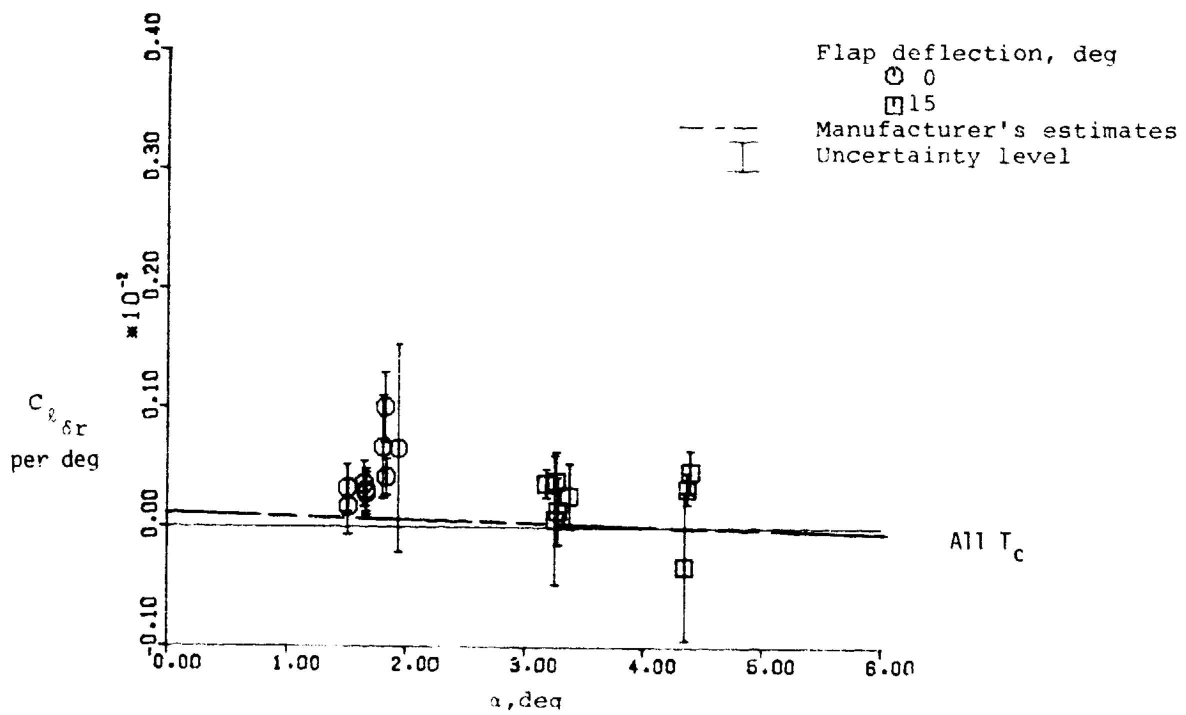

(e) $C_{n_{\delta_r}}$, $C_{\ell_{\delta_r}}$

Figure 7. Continued.

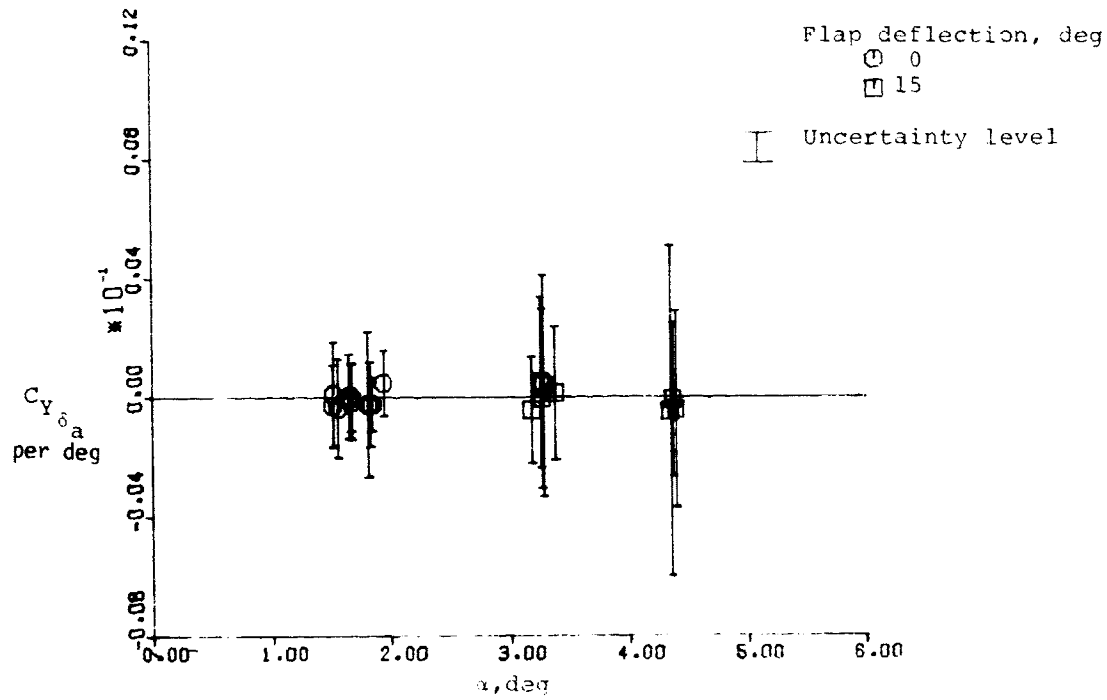

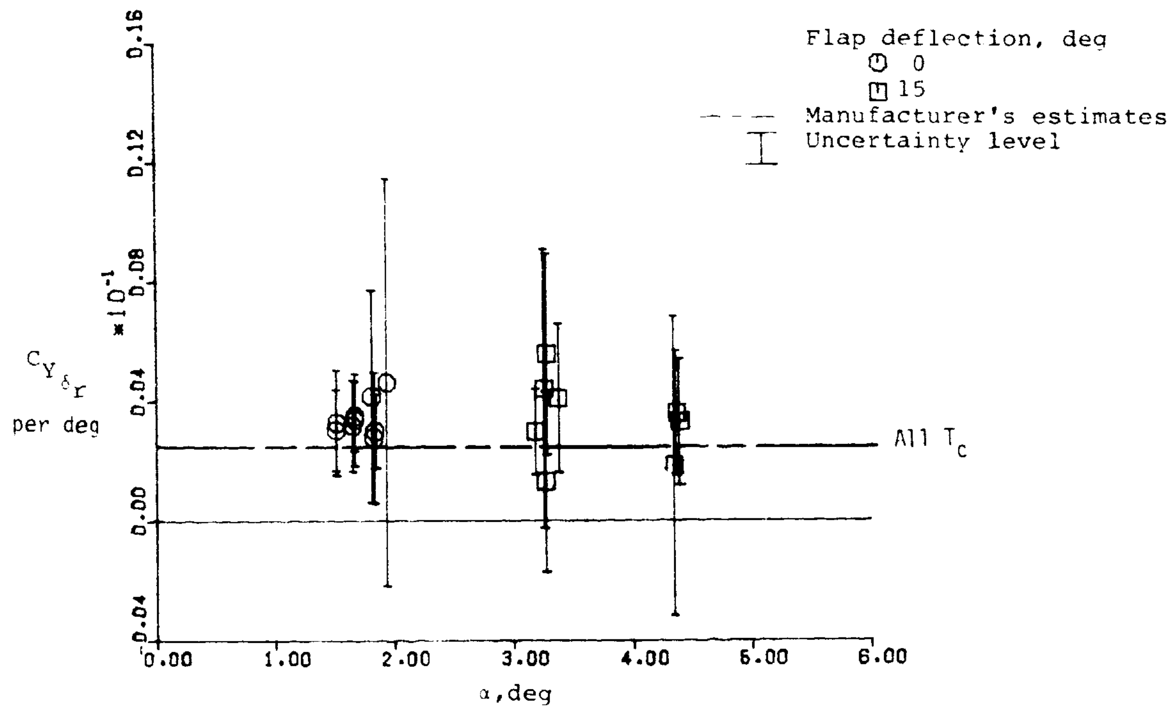

(f) $C_{Y_{\delta_a}}$, $C_{Y_{\delta_r}}$

Figure 7. Continued.

ORIGINAL PAGE IS
OF POOR QUALITY

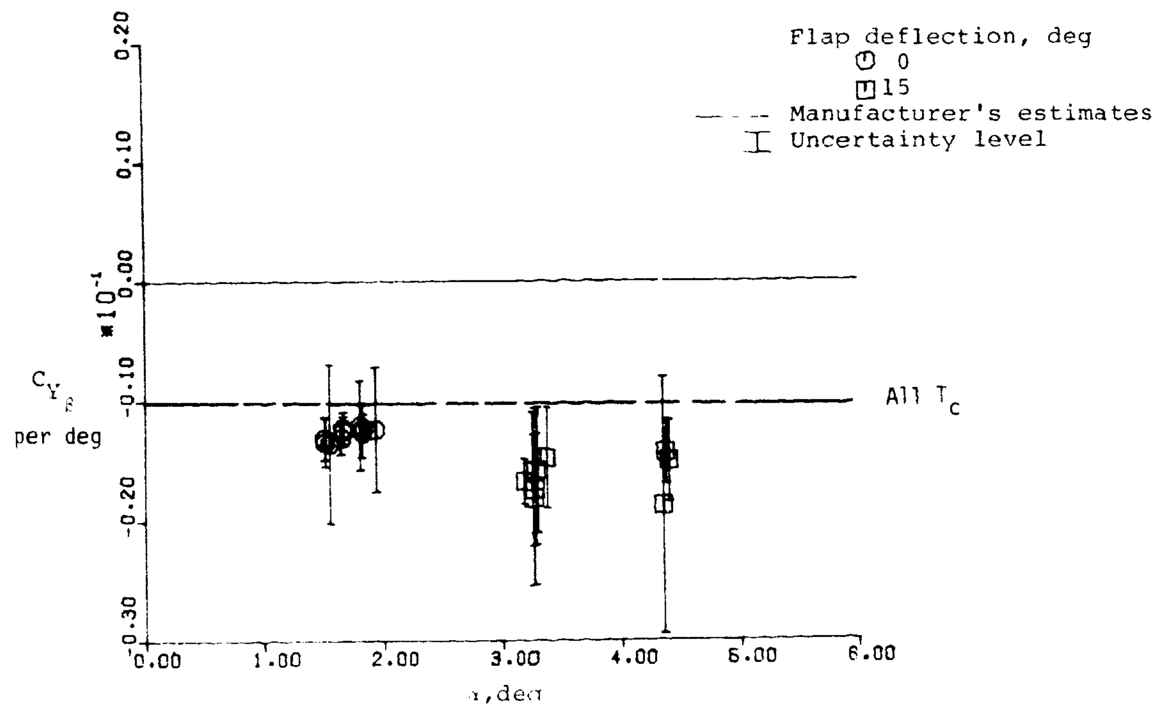

(g) C_{Y_β}

Figure 7. Concluded.

END

DATE

FILMED

MAY 22 1979